

# Small Hydrocarbon Cyclophanes: Synthesis, X-ray Analysis and Molecular Modelling

Tanja Lahtinen,<sup>[a]</sup> Elina Wegelius,<sup>[a]</sup> Juha Linnanto,<sup>[a]</sup> and Kari Rissanen\*<sup>[a]</sup>

**Keywords:** Cyclophanes / Pyrolysis / Prismands / Fused-ring systems / Molecular modeling

Small hydrocarbon cyclophanes, such as [2.2.0]*m,m*-cyclophane (**20**) and [2.2.0]*p,m,m*-cyclophane (**21**), are strained analogues of the well-known  $\pi$ -prismand [2.2.2]*p,p,p*-cyclophane (**1**). The synthetic route to these molecules is based on well-established cyclophane methodology which offers a general access to a whole family of hydrocarbon cyclophanes. Single crystal X-ray analysis and molecular model-

ling showed that the reduction of the ring size from 18-membered (**1**) to 14-membered (**21**) or 13-membered (**20**) has a substantial effect on the size and the shape of the cyclophane's cavity, thus blocking its ability to complex  $\text{Ag}^+$  ions.

(© Wiley-VCH Verlag GmbH, 69451 Weinheim, Germany, 2002)

## Introduction

Cyclophanes play a significant role in supramolecular chemistry, which is one of the fastest developing areas in modern chemistry.<sup>[1]</sup> Supramolecular chemistry is based on weak, often reversible, noncovalent interactions, holding together supramolecular complexes.<sup>[2]</sup> Among these interactions are hydrogen bonding, ion pairing, metal-to-ligand attractions,  $\pi$ -acid to  $\pi$ -base interactions, van der Waals attractions and cation- $\pi$  interactions. The very same interactions control the molecular recognition processes in biological systems.<sup>[3]</sup>

Some  $\pi$ -systems containing hydrocarbon cyclophanes can complex certain metal cations by interacting with the  $\pi$ -electron system of the hydrocarbon. This complexation is based on electron transfer between the aromatic moiety and positively charged metal cation.<sup>[4]</sup> Hydrocarbon cyclophanes like [2.2.2]*p,p,p*-cyclophane (**1**) which can form crystalline silver cation complexes are known as  $\pi$ -prismands.<sup>[5]</sup>

[2.2.2]*p,p,p*-Cyclophane (**1**), the first known  $\pi$ -prismand, forms an extraordinarily stable 1:1 complex **3** (Figure 1) with silver triflate where the  $\text{Ag}^+$  ion is located on the three-fold axis, 0.23 Å outside of the  $\pi$ -prismand cavity.<sup>[6]</sup> Another very interesting  $\pi$ -prismand was synthesised by Bokelheide et al.<sup>[6]</sup> They studied gas-phase dimerization of benzocyclobutenes in a stream of nitrogen and found that increasing the concentration of benzo[1,2:4,5]dicyclobutene in the hot zone of the pyrolysis tube produced [2<sub>6</sub>](1,2,4,5)cyclophane (**2**) named by the authors as deltaphane (Figure 1).<sup>[6,7]</sup> The rigid geometry of deltaphane, with its internal cavity surrounded by three benzene rings, seemed ideal for metal ion complexation of

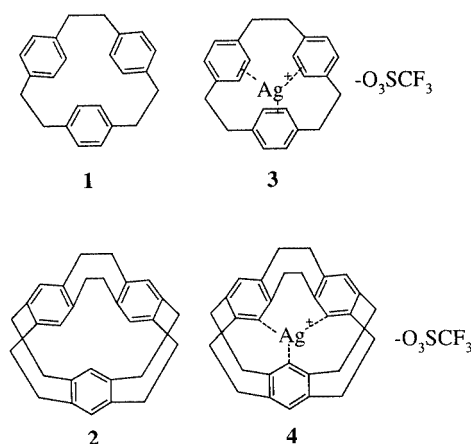


Figure 1. [2.2.2]*p,p,p*-Cyclophane (**1**), [2<sub>6</sub>](1,2,4,5)cyclophane (**2**) and their silver complexes **3** and **4**

the  $\pi$ -prismand type. Although deltaphane itself is essentially insoluble in tetrahydrofuran, it rapidly dissolves in tetrahydrofuran in the presence of silver triflate to form complex **4** (Figure 1). In both hydrocarbons **1** and **2** all three benzene rings are arranged with face-to-face symmetry giving the structure which is considered as an ideal  $\pi$ -prismand.<sup>[6,7]</sup>

Concave hydrocarbon cyclophanes have been shown to be able to extract certain metal ions from the aqueous phase into a nonpolar phase.<sup>[8]</sup> A number of spherical hydrocarbons have been tested, and among these the concave hydrocarbon [2.2.2]*p,p,p*-cyclophane (**1**) was found to extract  $\text{Ag}^+$  to a much greater extent than alkali metal ions,  $\text{Tl}^+$  or  $\text{Hg}^{2+}$ . This complexation selectivity could be used in applications such as ion-selective electrodes.<sup>[8]</sup>

Previously, we have reported the synthesis of a family of small hydrocarbon cyclophanes which are either isomeric

<sup>[a]</sup> Department of Chemistry, University of Jyväskylä, P. O. Box 35, Surfontie 9, 40351 Jyväskylä, Finland

structures or strained analogues of the well-known [2.2.2]*p,p,p*-cyclophane (**1**). Our aim is to study how strained a molecule can be and still act as a  $\pi$ -prism and form a stable complex with silver cation.<sup>[9–11]</sup>

Sulfone pyrolysis was selected as a suitable synthetic method due to the unsymmetrical nature of these hydrocarbon cyclophanes. This procedure is one of the most important applications in cyclophane chemistry as it offers access to a large diversity of macrocycles.<sup>[12,13]</sup>

Figure 2 presents the two isomeric structures of [2.2.2]*p,p,p*-cyclophane (**1**) namely, [2.2.2]*m,m,p*-cyclophane (**5**) and [2.2.2]*m,p,p*-cyclophane (**6**) and the two slightly strained analogues, namely [2.2.1]*m,p,p*-cyclophane (**7**) and [2.2.1]*p,p,p*-cyclophane (**8**), prepared by us.<sup>[9–11]</sup>

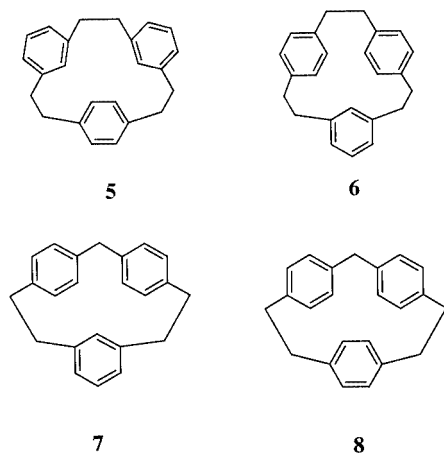


Figure 2. [2.2.2]*m,m,p*-Cyclophane (**5**), [2.2.2]*m,p,p*-cyclophane (**6**), [2.2.1]*m,p,p*-cyclophane (**7**) and [2.2.1]*p,p,p*-cyclophane (**8**)

We have surveyed the complexation abilities of the hydrocarbon cyclophanes **5**, **6**, **7** and **8** by using the same procedure that Pierre et al.<sup>[5]</sup> used for the parent [2.2.2]*p,p,p*-cyclophane (**1**). All [2.2.2]cyclophanes and [2.2.1]cyclophanes presented in Figure 2 are able to complex silver triflate due to electron transfer between their double bonds and the positively charged metal cation, producing  $\pi$ -prism and complexes (Figure 3). The single crystal X-ray analysis of cyclophane complexes **9**, **10**, **11** and **12** showed that the sil-

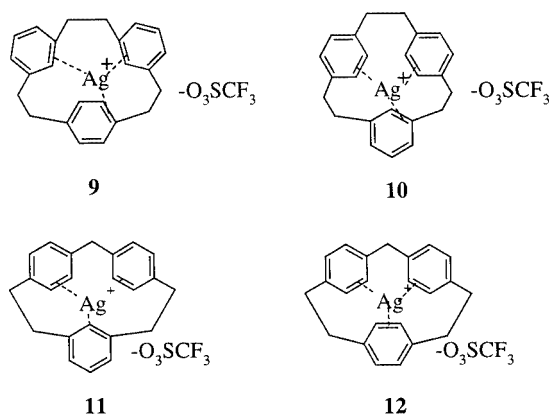


Figure 3. Ag-triflate complexes **9**, **10**, **11** and **12**

ver cation is located outside of the  $\pi$ -prism and cavity, as in the known [2.2.2]*p,p,p*-cyclophane- (**3**) and deltaphane- $\text{Ag}^+$  complexes (**4**).<sup>[9–11]</sup>

We were also interested to study if the cyclophane hydrocarbons could act as ionophores. Four structurally similar cyclophanes, i.e. [2.2.2]*p,p,p*-cyclophane (**1**), [2.2.2]*m,p,p*-cyclophane (**6**), [2.2.1]*m,p,p*-cyclophane (**7**) and [2.2.1]*p,p,p*-cyclophane (**8**) were studied as  $\pi$ -coordinating ionophores in solvent membrane-based ion-selective electrodes (ISEs).<sup>[14,15]</sup> The selectivity of the ISEs to  $\text{Ag}^+$  was found to depend on both the symmetry and the formal ring size of the cyclophanes, indicating that the cation- $\pi$  interactions involved are very sensitive to the spatial organisation of the  $\pi$ -coordinating benzene rings in the ionophores. Thus, ISEs based on *p,p,p*-cyclophanes **1** and **8** showed a significantly higher selectivity for  $\text{Ag}^+$  than the corresponding *m,p,p*-cyclophanes **6** and **7**. The structure of the [2.2.2]*p,p,p*-cyclophane (**1**) ionophore seems to be particularly favourable for  $\text{Ag}^+$ - $\pi$  interactions, resulting in ISEs with the best  $\text{Ag}^+$  selectivity among the cyclophanes studied.<sup>[14,15]</sup>

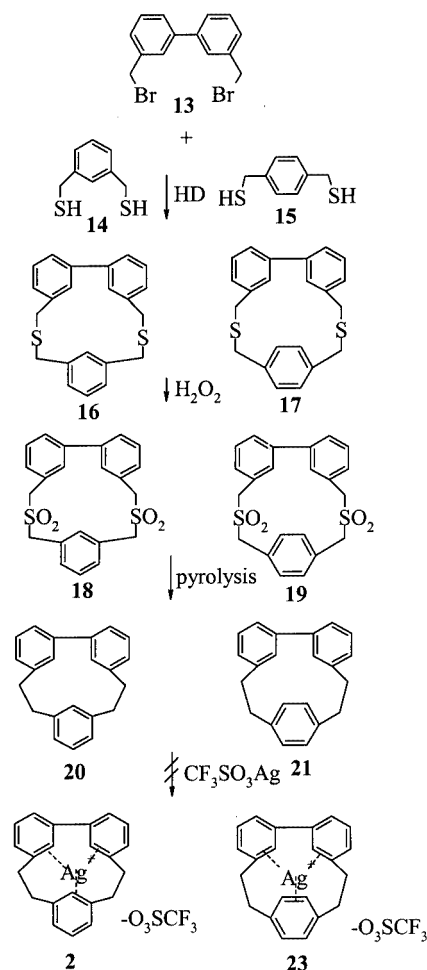
The nature of the bonding in  $\pi$ -prism and the conformations of [2.2.2]cyclophanes and [2.2.1]cyclophanes has been estimated by ab initio Hartree–Fock (HF) and DFT MO calculations.<sup>[16,17]</sup> These calculations indicated that [2.2.2]cyclophanes are flexible and the ethane bridges allow twisting, meaning that [2.2.2]cyclophanes are capable of adopting various conformations when complexed with  $\text{Ag}^+$ . In comparison to [2.2.2]cyclophanes the [2.2.1]cyclophanes possess a more strained structure and are capable of fewer conformations. However, despite this increased rigidity of [2.2.1]cyclophanes they still have only small energy differences between the different conformations and thus are capable of varying their conformation when complexing with metal ions.<sup>[16,17]</sup>

Following the syntheses and testing of [2.2.1]cyclophanes, we were extremely interested to study even smaller and more strained hydrocarbon cyclophanes, i.e. [2.2.0]*m,m,m*-cyclophane (**20**)<sup>[18]</sup> and [2.2.0]*p,m,m*-cyclophane (**21**)<sup>[19]</sup> to see if even more rigid and distorted cyclophanes than [2.2.1]cyclophanes can act as  $\pi$ -prism and. In this work we report the synthesis of [2.2.0]*m,m,m*-cyclophane (**20**)<sup>[18]</sup> and [2.2.0]*p,m,m*-cyclophane (**21**)<sup>[19]</sup> and five new crystal structures, including sulfides **16** and **17**, sulfone **18**, hydrocarbon **21** and from the [2.2.2]cyclophane hydrocarbon family the [2.2.2]*m,p,p*-cyclophane **5** (Figure 2). We also report molecular orbital calculations on hydrocarbons [2.2.0]*m,m,m*-cyclophane (**20**) and [2.2.0]*p,m,m*-cyclophane (**21**).

## Results and Discussion

### Synthesis

The three step synthesis (Scheme 1) of [2.2.0]*m,m,m*-cyclophane (**20**)<sup>[18]</sup> and [2.2.0]*p,m,m*-cyclophane (**21**)<sup>[19]</sup> is based on well-known cyclophane methodology, where a sulfide cyclisation is performed under high dilution conditions followed by oxidation and sulfone pyrolysis.<sup>[12,13]</sup>



Scheme 1

The high-dilution cyclisations to form 1,10-dithia-[3.3.0]*m,m*-cyclophane (**16**; 69% yield) and 1,10-dithia-[3.3.0]*p,m*-cyclophane (**17**; 66% yield) were performed starting from 3,3'-bis(bromomethyl)-1,1'-biphenyl (**13**) and either (1,3-phenylene)bis(methanethiol) (**14**) or (1,4-phenylene)bis(methanethiol) (**15**), with toluene as solvent. The cyclic disulfides **16** and **17** were oxidized by  $\text{H}_2\text{O}_2$  under reflux to 1,10-dithiatetroxide[3.3.0]*m,m,m*-cyclophane (**18**; 37%) and 1,10-dithiatetroxide[3.3.0]*p,m,m*-cyclophane (**19**; 38%), respectively. The disulfides were identified by IR spectroscopy which showed strong adsorption in the  $\text{SO}_2$  region ( $1100\text{--}1330\text{ cm}^{-1}$ ). The disulfones **18** and **19** were pyrolysed to the hydrocarbons [2.2.0]*m,m,m*-cyclophane (**20**) and [2.2.0]*p,m,m*-cyclophane (**21**), respectively, with a ring oven pyrolysis apparatus at  $600\text{--}620\text{ }^\circ\text{C}$  and  $2 \times 10^{-5}\text{--}8 \times 10^{-6}\text{ mbar}$ . The yield after isolation was 50% for **20** and 58% for **21**. To study the complexation ability of ligands **20** and **21**, equimolar amounts of free ligand and silver triflate were mixed using the same procedure as Pierre et al.<sup>[5]</sup> No complexation was detected.

### X-ray Crystallography and Molecular Modelling

After extensive attempts to grow crystals of all the synthesised molecules five new X-ray structures were obtained.

A member of the earlier reported family of hydrocarbon [2.2.2]cyclophanes,<sup>[9,10]</sup> namely [2.2.2]*m,m,p*-cyclophane (**5**) formed crystals by slow evaporation of a 1:1 dichloromethane/hexane mixture. Colourless crystals of the disulfides (**16** and **17**) were obtained by dissolving the crude products in dichloromethane and allowing the solvent to evaporate very slowly from each solution at room temperature, to give small well-diffracting crystals of **16** and **17**. Disulfone cyclophanes are typically highly insoluble in any solvents, thus getting a crystal structure of those is very difficult. However, fortunately a small amount of disulfone **18** present as an impurity in an NMR tube (in  $\text{CDCl}_3$ ) containing hydrocarbon **20** crystallised out. Crystals of hydrocarbon cyclophane **21** were obtained by slow evaporation of a dichloromethane solution. The crystal data and refinement details of all these compounds are given in Table 1.

The hydrocarbon [2.2.2]*m,m,p*-cyclophane (**5**) crystallises in an acentric monoclinic space group ( $P2_1$ ) with two slightly different molecules (one of them highly disordered) in the asymmetric unit. The X-ray structure (Figure 4) shows a very similar conformation to that present in the earlier hydrocarbon [2.2.2]cyclophanes.<sup>[5,9,10]</sup> The X-ray structure of its  $\pi$ -prismant  $\text{Ag}^+$  complex **9** has been reported earlier.<sup>[9,10]</sup> X-ray structures of similar cyclophane silver complexes have been reported by Hopf et al.<sup>[20–23]</sup>

Disulfides **16** and **17** crystallise in a monoclinic space group ( $P2_1/n$ ). The structures are strained and forced almost planar due to the very strained diphenyl parts of the molecules (Figure 5 and 6). Disulfone **18** (Figure 7) crystallises in a monoclinic space group ( $P2_1/c$ ), and shows only a slight conformational change from the disulfide **16**. The target hydrocarbon cyclophane **21** (Figure 8) crystallises in a triclinic space group ( $P\bar{1}$ ). The structure of hydrocarbon **21** is highly strained due to the biphenyl part of the molecule. The angles in [2.2.0]*p,m,m*-cyclophane (**21**) for the best least-squares planes through the aromatic rings are  $161.6(1)^\circ$ ,  $50.8(1)^\circ$  and  $53.1(1)^\circ$ . The same angles in [2.2.2]*p,p,p*-cyclophane (**1**) are  $61.2(1)^\circ$ ,  $61.5(1)^\circ$  and  $60.4(1)^\circ$  indicating an almost ideal  $\pi$ -prismant geometry and a triangular shape. In [2.2.0]*p,m,m*-cyclophane (**21**) the typical  $\pi$ -prismant face-to-face structure is forced to collapse and the flexibility between the aromatic rings that makes it possible to adapt various conformations is lost.

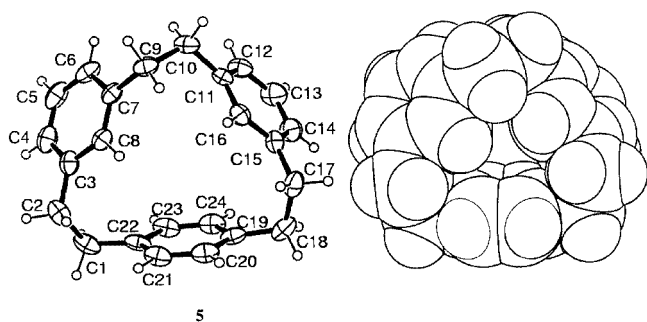
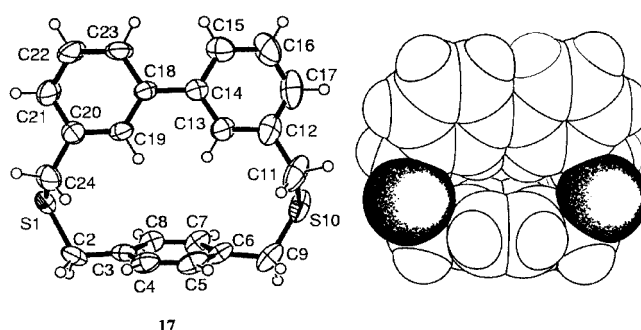
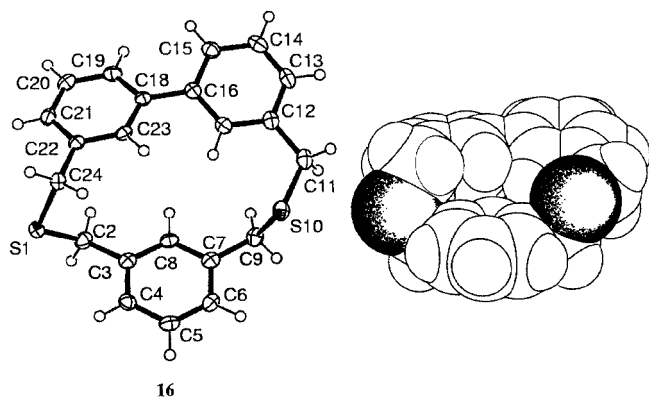
### Molecular Orbital Calculations

The starting geometries of [2.2.0] *m,m,m*-cyclophane (**20**) and [2.2.0] *p,m,m*-cyclophane (**21**) were fully optimized at the semi-empirical PM3<sup>[24]</sup> level on a Silicon Graphics O2 workstation by using SPARTAN software.<sup>[25]</sup> Geometry optimisations were then continued on an AlphaServer ES-40 workstation at the ab initio HF/6–31G\* and density functional B3LYP/6–31G\* levels with Gaussian98 software.<sup>[26]</sup>

Both of the methods used, B3LYP/6–31G\* and HF/6–31G\*, give almost identical optimised structures. Some selected bond and torsion angles of the most stable conformations of the B3LYP-optimised cyclophanes are shown with the experimental values obtained from X-ray analysis in Table 2. These calculated bond parameters agree well

Table 1. Crystal data and experimental details for **5**, **16**, **17**, **18** and **21**

Compound	5	16	17	18	21
Formula	C <sub>24</sub> H <sub>24</sub>	C <sub>22</sub> H <sub>20</sub> S <sub>2</sub>	C <sub>22</sub> H <sub>20</sub> S <sub>2</sub>	C <sub>22</sub> H <sub>20</sub> S <sub>2</sub> O <sub>4</sub>	C <sub>22</sub> H <sub>20</sub>
Crystal system	monoclinic	monoclinic	monoclinic	monoclinic	triclinic
Space group	<i>P</i> 2 <sub>1</sub>	<i>P</i> 2 <sub>1</sub> / <i>n</i>	<i>P</i> 2 <sub>1</sub> / <i>n</i>	<i>P</i> 2 <sub>1</sub> / <i>c</i>	<i>P</i> $\bar{1}$
<i>M<sub>r</sub></i>	312.4	348.5	348.5	412.5	284.4
<i>a</i> (Å)	10.3419(4)	12.7237(5)	16.5290(5)	10.6792(3)	8.6888(9)
<i>b</i> (Å)	10.8827(4)	6.9382(5)	5.3933(2)	8.6973(2)	9.3445(9)
<i>c</i> (Å)	16.0015(5)	19.8146(12)	21.2731(8)	21.1205(7)	10.3214(12)
$\alpha$ (°)	90	90	90	90	77.888(7)
$\beta$ (°)	90.914(1)	100.691(4)	111.503(1)	104.5285(12)	73.150(6)
$\gamma$ (°)	90	90	90	90	77.694(7)
<i>V</i> (Å <sup>3</sup> )	1800.7(1)	1718.9(2)	1764.4(1)	1898.8(2)	773.7(1)
<i>Z</i>	4	4	4	4	2
<i>D<sub>c</sub></i> (Mg·m <sup>-3</sup> )	1.152	1.347	1.312	1.443	1.221
$\mu$ (mm <sup>-1</sup> )	0.065	0.309	0.301	0.307	0.069
Refl. Measured/unique	8775/5688	7967/3034	9214/3326	9824/3357	5842/2686
Refl. used in refinement	5208	2422	2383	2252	1972
[ <i>I</i> > 2 $\sigma$ ( <i>I</i> )]					
<i>R<sub>int</sub></i>	0.021	0.046	0.075	0.078	0.048
<i>R</i> [ <i>I</i> > 2 $\sigma$ ( <i>I</i> )]	0.039	0.043	0.079	0.049	0.046
<i>wR</i> <sup>2</sup> [ <i>I</i> > 2 $\sigma$ ( <i>I</i> )]	0.089	0.084	0.163	0.091	0.100

Figure 4. The X-ray structure of **5**Figure 6. X-ray Structure of **17**Figure 5. X-ray structure of **16**

with previously reported values in similar cyclophanes,<sup>[16,17]</sup> and are also in very good agreement with experimental X-ray values.

Based on the very good agreement between the calculated structure and the X-ray structure for **21**, the calculated structure presented here for [2.2.0] *m,m,m*-cyclophane (**20**) (Figure 9) can be accepted as a good model of its structure,

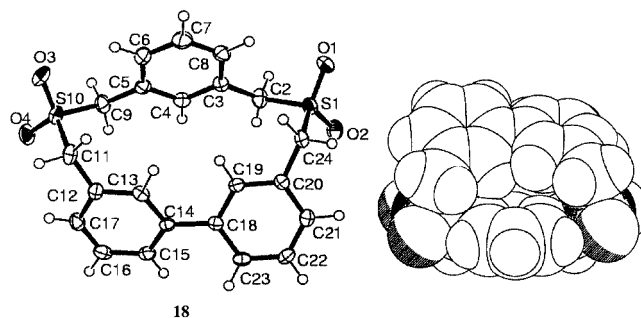
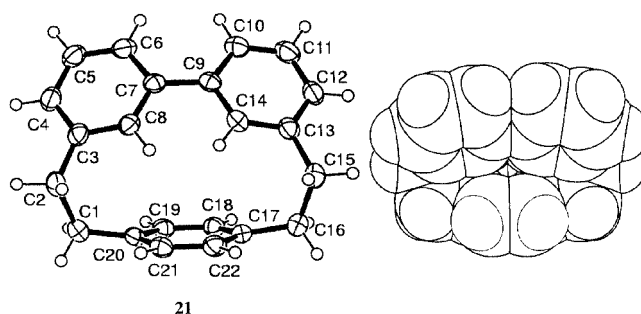
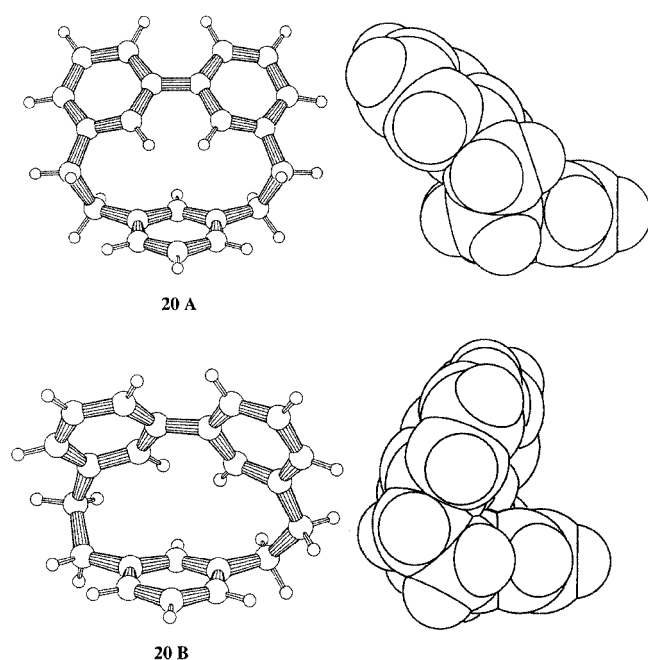
Figure 7. X-ray Structure of **18**Figure 8. X-ray Structure of **21**



Table 2. Selected bond and torsion angles [°]

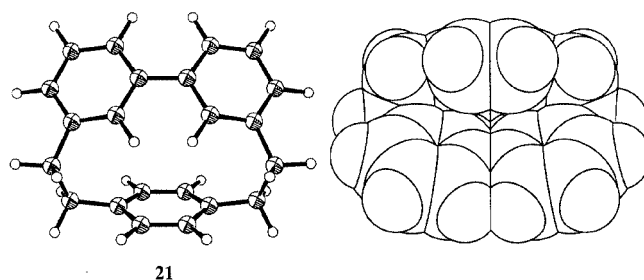
Atoms <sup>[a]</sup>	20	21	21, exp. (X-ray)
C2–C1–C20	114.3	114.0	114.9
C1–C2–C3	112.4	113.4	115.0
C15–C16–C18	114.3	—	—
C15–C16–C17	—	114.0	114.6
C13–C15–C16	112.4	113.4	115.3
C17–C16–C15–C13	–78.5	–56.9	–54.9
C13–C15–C16–C18	78.5	—	—
C3–C2–C1–C20	—	56.9	56.2
C8–C7–C9–C14	–0.1	–0.1	–2.4
C15–C16–C17–C22	–68.9	–67.0	–68.4
C16–C15–C13–C12	–116.7	–105.7	–111.2
C1–C2–C3–C4	116.7	105.7	113.8
C2–C1–C20–C21	68.9	—	—

<sup>[a]</sup> Numbering according to Figure 8.

Figure 9. The calculated (B3LYP/6–31G\*) structures for **20**

the experimental structure of which is not available. The calculations result in two different conformations for the [2.2.0] *m,m,m*-cyclophane (**20**) and come from the different orientation of the *meta*-substituted benzene ring. The energy difference between these conformers is about 7 kcal/mol (Figure 9), the A conformer being the more favoured.

Figure 10 shows the most stable calculated structure for [2.2.0] *p,m,m*-cyclophane (**21**). In this structure the orientation of the benzene rings is similar and agrees very well with the experimental X-ray structure. In all the calculated structures for **20** and **21**, the  $\pi$ -prismant cavity is too small to complex metal ions or small molecules, differing substantially from the  $\pi$ -prismant [2.2.2]- and [2.2.1]cyclophanes.<sup>[9–11]</sup> This difference originates from the structure of [2.2.0]cyclophane itself. In the [2.2.2]cyclophanes all the aromatic rings are connected together via ethane bridges, whereas in [2.2.0]cyclophanes two out of the three aromatic

Figure 10. The calculated (B3LYP/6–31G\*) structure for **21**

rings are part of a much more rigid biphenylene moiety resulting in a collapsed and rigid structure incapable of acting as a  $\pi$ -prismant.

## Conclusion

We have recently synthesised and tested a group of hydrocarbon cyclophanes namely [2.2.2]-, [2.2.1]- and [2.2.0]cyclophanes in order to survey the limits of  $\pi$ -prismant behaviour and compared those to known  $\pi$ -prismants such as [2.2.2]*p,p,p*-cyclophane (**1**) and deltaphane (**2**). The reduction of the ring size from [2.2.2]cyclophanes to [2.2.0]cyclophanes and the *para/meta* coupling of the phenyl rings seems to have a considerable impact on the complexing ability. In particular, in the [2.2.2]cyclophanes, which have a larger ring size than [2.2.1]cyclophanes, the spatial organisation of the benzene rings influences the selectivity of the cyclophanes.

In the case of the [2.2.0]cyclophanes **20** and **21**, in all the calculated structures — this is confirmed by the X-ray structure of **21** — the  $\pi$ -prismant cavity is too small to complex metal atoms or small molecules and differs in this way from [2.2.2]- and [2.2.1]cyclophanes. Although [2.2.1]cyclophanes are more strained than [2.2.2]cyclophanes they still have only a small energy difference between the conformations and thus are capable of adopting different conformations when complexing with metal ions. In the structures of [2.2.0]cyclophanes the inability to complex  $\text{Ag}^+$  ions originates from the structure of the cyclophane. The [2.2.2]cyclophane structures have a triangular orientation of three perpendicular benzene rings and a large enough cavity for the complexation. In the [2.2.0]cyclophanes the structure is too collapsed, due to the biphenyldiyl moiety, and the adoption of a suitable conformation for the cation  $\pi$ -interactions needed for the  $\pi$ -prismant behaviour is not possible.

## Experimental Section

**1,10-Dithia[3.3.0]*m,m,m*-cyclophane (**16**):**<sup>[18]</sup> A solution of 3,3'-bis-(bromomethyl)-1,1'-biphenyl (**13**) (255.0 mg, 0.750 mmol) and 1,3-di(thiomethyl)benzene (**14**) (125.0 mg, 0.750 mmol) in 100 mL of toluene and a solution of 113.0 mg of KOH in 100 mL of abs. ethanol were added dropwise to 250 mL of refluxing toluene under an inert gas atmosphere in a period of 4 h. After the addition the

mixture was refluxed for an additional 3 h and then cooled to room temperature. The inorganic solid material was filtered and the solvent was evaporated off. The residue was dissolved in a small amount of chloroform and filtered through silica gel. The solvent was evaporated to yield a pale yellow solid product. For the X-ray analysis the crude product was recrystallised from dichloromethane yielding colourless needles. Yield 181.0 mg (69%).  $^1\text{H}$  NMR (500 MHz,  $\text{CDCl}_3$ ):  $\delta$  = 3.51 (s, 4 H), 3.71 (s, 4 H), 6.99–7.42 (m, 12 H) ppm.  $^{13}\text{C}$  NMR (126 MHz,  $\text{CDCl}_3$ ):  $\delta$  = 34.72, 34.89, 123.25, 125.88, 126.48, 127.35, 128.07, 128.15, 128.90, 137.28, 137.95, 138.34 ppm. GC-MS (EI)  $\text{C}_{22}\text{H}_{20}\text{S}_2$  (348.5):  $m/z$  (%) = 348 (55).

**1,10-Dithia[3.3.0]*p,m,m*-cyclophane (17):**<sup>[19]</sup> A solution of 3,3'-bis-(bromomethyl)-1,1'-biphenyl (**13**) (255.0 mg, 0.750 mmol) and 1,3-di(thiomethyl)benzene (**15**) (125.0 mg, 0.750 mmol) in 100 mL of toluene and a solution of 113.0 mg of KOH in 100 mL of abs. ethanol were added dropwise to 250 mL of refluxing toluene under an inert gas atmosphere in a period of 4 h. After that the mixture was refluxed for an additional 2 h and then cooled to room temperature. The inorganic solid material was filtered and the solvent was evaporated off. The residue was dissolved in a small amount of chloroform and filtered through silica gel. The solvent was evaporated to yield a pale yellow solid product. For the X-ray analysis the crude product was recrystallised from dichloromethane yielding colourless needles. Yield 173.0 mg (66%).  $^1\text{H}$  NMR (500 MHz,  $\text{CDCl}_3$ ):  $\delta$  = 3.78 (s, 4 H), 3.91 (s, 4 H), 6.51 (s, 2 H), 7.09–7.42 (m, 10 H) ppm.  $^{13}\text{C}$  NMR (126 MHz,  $\text{CDCl}_3$ ):  $\delta$  = 37.17, 38.50, 124.82, 127.02, 128.02, 128.33, 129.08, 138.78, 139.64, 140.56 ppm. GC-MS (EI)  $\text{C}_{22}\text{H}_{20}\text{S}_2$  (348.5):  $m/z$  (%) = 348 (71%).

**1,10-Dithiatetroxide[3.3.0]*m,m,m*-cyclophane (18):**<sup>[18]</sup> 1,10-Dithia-[3.3.0]*m,m,m*-cyclophane (**16**) (300.0 mg, 0.860 mmol), 16 mL of glacial acetic acid and 8 mL of toluene were mixed together and heated to reflux. After that 2 mL of 35%  $\text{H}_2\text{O}_2$  was added and refluxed for an additional hour. The addition of  $\text{H}_2\text{O}_2$  and 1 h refluxing was repeated three times. After cooling to room temperature the mixture was filtered and the white solid material was washed a few times with glacial acetic acid. The product was used for the following reaction without any further purification. Yield 132.0 mg (37%). IR (KBr):  $\tilde{\nu}$  = 1300–1100  $\text{cm}^{-1}$  ( $\text{SO}_2$ ). GC-MS (EI)  $\text{C}_{22}\text{H}_{20}\text{S}_2\text{O}_4$  (412.5):  $m/z$  (%) = 412 (47%).

**1,10-Dithiatetroxide[3.3.0]*p,m,m*-cyclophane (19):**<sup>[19]</sup> 1,10-Dithia-[3.3.0]*p,m,m*-cyclophane (**17**) (200.0 mg, 0.570 mmol), 11 mL of glacial acetic acid and 5 mL of toluene were mixed together and heated to reflux. After that 1 mL of 35%  $\text{H}_2\text{O}_2$  was added and refluxed for an additional hour. The addition of  $\text{H}_2\text{O}_2$  and 1 h refluxing was repeated three times. After cooling to room temperature the mixture was filtered and the white solid material was washed a few times with glacial acetic acid. The product was used for the following reaction without any further purification. Yield 89.0 mg (38%). IR (KBr):  $\tilde{\nu}$  = 1300–1100  $\text{cm}^{-1}$  ( $\text{SO}_2$ ). GC-MS (EI)  $\text{C}_{22}\text{H}_{20}\text{S}_2\text{O}_4$  (412.5):  $m/z$  (%) = 412 (18%).

**[2.2.0]*m,m,m*-Cyclophane (20):**<sup>[18]</sup> 1,10-Dithiatetraoxide[3.3.0]-*m,m,m*-cyclophane (**18**) (50.0 mg, 0.121 mmol) was placed in a quartz tube and heated to 600 °C under high vacuum ( $7.64 \times 10^{-6}$  mbar) in a pyrolysis apparatus. During the heating the product condensed at the other end of the tube. After 5 h the tube was left to cool to room temperature and the pale yellow product was then extracted from the tube with dichloromethane. The solvent was evaporated to yield a pale yellow solid product. Yield 17.4 mg (50%), m.p.: 100–101 °C (ref.<sup>[18]</sup> 100–101 °C).  $^1\text{H}$  NMR (500 MHz,  $\text{CDCl}_3$ ):  $\delta$  = 2.77–3.35 (m, 8 H), 6.93 (s, 2 H), 7.09 (d,

2 H), 7.16 (s, 1 H), 7.22 (d, 2 H), 7.24 (t, 2 H), 7.30 (d, 2 H), 7.34 (t, 1 H) ppm.  $^{13}\text{C}$  NMR (126 MHz,  $\text{CDCl}_3$ ):  $\delta$  = 34.53, 35.26, 122.23, 125.71, 126.82, 127.79, 129.82, 132.69, 135.88, 140.85, 141.86, 142.43 ppm. HRMS:  $m/z$  ( $\text{M}^+$ ,  $\text{C}_{22}\text{H}_{20}$ ): calcd: 284.156501; found 284.156338.

**[2.2.0]*p,m,m*-Cyclophane (21):**<sup>[19]</sup> 1,10-Dithiatetraoxide[3.3.0]*p,m,m*-cyclophane (**19**) (50.9 mg, 0.123 mmol) was placed in a quartz tube and heated to 600 °C under high vacuum ( $1.46 \times 10^{-5}$  mbar) in a pyrolysis apparatus. During the heating the product condensed at the other end of the tube. After 3 h the tube was left to cool to room temperature and the white product was then extracted from the tube with dichloromethane. The solvent was evaporated to yield a white solid product. The product was recrystallised from dichloromethane yielding well diffracting colourless needles. Yield 20.3 mg (58%), m.p.: 150–151 °C (ref.<sup>[19]</sup> 165–166 °C).  $^1\text{H}$  NMR (500 MHz,  $\text{CDCl}_3$ ):  $\delta$  = 2.87–2.97 (m, 8 H), 6.23 (s, 2 H), 6.85 (s, 4 H), 7.03 (d, 2 H), 7.23 (t, 2 H), 7.41 (d, 2 H) ppm.  $^{13}\text{C}$  NMR (126 MHz,  $\text{CDCl}_3$ ):  $\delta$  = 36.95, 37.40, 121.96, 126.24, 128.28, 130.29, 130.81, 137.39, 139.65, 139.68 ppm. HRMS  $m/z$  ( $\text{M}^+$ ,  $\text{C}_{22}\text{H}_{20}$ ): calcd: 284.156501; found 284.156444.

**[2.2.0]*m,m,m*-Cyclophane-Ag-triflate (22):** A solution of [2.2.0]*m,m,m*-cyclophane (**20**) (11.6 mg, 0.041 mmol) in dichloromethane was added to solution of silver triflate (10.5 mg, 0.041 mmol) in THF. The mixture was stirred and allowed to evaporate very slowly to dryness in darkness at room temperature to give a brown solid product. No complexation was detected.

**[2.2.0]*p,m,m*-Cyclophane-Ag-triflate (23):** A solution of [2.2.0]*p,m,m*-cyclophane (**21**) (11.6 mg, 0.041 mmol) in dichloromethane was added to a solution of silver triflate (10.5 mg, 0.041 mmol) in THF. The mixture was stirred and allowed to evaporate very slowly to dryness in darkness at room temperature to give a whitish crystalline powder. No complexation was detected.

**Crystal Structure Analysis:** Data were recorded with a Nonius Kappa CCD diffractometer using graphite monochromatised  $\text{Mo-K}\alpha$  ( $\lambda$  = 0.71073 Å) radiation,  $T$  = 173.0(1) K. The data were processed with *Denzo* (Z. Otwinowski and W. Minor, Methods in Enzymology, Volume 276: Macromolecular Crystallography, part A, p.307–326, 1997, C. W. Carter Jr. & R. M. Sweet, Eds., Academic Press). Lorentz-polarisation corrections were applied. Structure solutions were performed by direct methods (G. M. Sheldrick, SHELXS-97: *A Program for Automatic Solution of Crystal Structures*, University of Göttingen, Germany, 1997) and refinements<sup>25</sup> on  $F^2$  (G. M. Sheldrick, SHELXL-97: *A Program for Crystal Structure Refinement*, University of Göttingen, Germany, 1997). The hydrogen atoms were either calculated at their idealised positions with isotropic temp. factors (1.2- or 1.5-times the C temp. factor) and refined as riding atoms (the structures of **5** and **17**) or found from the electron density map and refined isotropically (**16**, **18** and **21**). In the case of structure **5** two crystallographically independent molecules were found in the asymmetric unit. In one of the molecules two aromatic rings and five bridging  $\text{CH}_2$  groups are disordered over two positions with occupancies of 0.45 and 0.55.

CCDC-181698 (**5**), -181699 (**16**), -181700 (**17**), -181701 (**18**) and -181702 (**21**) contain the supplementary crystallographic data for this paper. These data can be obtained free of charge at [www.ccdc.cam.ac.uk/conts/retrieving.html](http://www.ccdc.cam.ac.uk/conts/retrieving.html) [or from the Cambridge Crystallographic Data Centre, 12, Union Road, Cambridge CB2 1EZ, UK; Fax: (internat.) +44–1223/336–0333; E-mail: [deposit@ccdc.cam.ac.uk](mailto:deposit@ccdc.cam.ac.uk)].

## Acknowledgments

We warmly thank Ms. Mirja Lahtiperä for measuring the MS spectra and Mr. Reijo Kauppinen for running the NMR spectra.

- [1] F. Vögtle, *Cyclophane Chemistry*, Wiley, Chichester, **1993**.
- [2] E. Weber and F. Vögtle, in *Comprehensive Supramolecular Chemistry* (Eds.: J. L. Atwood, J. E. D. Davies, D. D. MacNicol and F. Vögtle), Vol. 2, Ch. 1, Pergamon, Exeter, **1996**.
- [3] D. J. Cram, *Angew. Chem. Int. Ed. Engl.* **1986**, *25*, 1039–1057.
- [4] F. Vögtle C. Seel and P.-M. Windscheif, in *Comprehensive Supramolecular Chemistry* (Eds.: J. L. Atwood, J. E. D. Davies, D. D. MacNicol and F. Vögtle), Pergamon, Oxford, **1996**, vol. 2, ch. 6.
- [5] J.-L. Pierre, P. Baret, P. Chautemps, M. Armand, *J. Am. Chem. Soc.* **1981**, *103*, 2986–2988.
- [6] H. C. Kang, A. W. Hanson, B. Eaton, V. J. Boekelheide, *J. Am. Chem. Soc.* **1985**, *107*, 1979–1985.
- [7] F. Vögtle, *Supramolecular Chemistry*, Wiley, Chichester, **1991**.
- [8] J. Gross, G. Harder, A. Siepen, J. Harren, F. Vögtle, H. stephen, K. Gloe, B. Ahlers, K. Cammann, K. Rissanen, *Chem. Eur. J.* **1996**, *2*, 1585–1595.
- [9] T. Seppälä, E. Wegelius, K. Rissanen, *New J. Chem.* **1998**, *22*, 789–791.
- [10] T. Lahtinen, E. Wegelius, K. Airola, E. Kolehmainen, K. Rissanen, *J. Prakt. Chem./Chem. Ztg.* **1999**, *341*, 237–244.
- [11] T. Lahtinen, E. Wegelius, K. Rissanen, *New J. Chem.* **2001**, *25*, 905–911.
- [12] J. Dohm, F. Vögtle, *Top. Curr. Chem.* **1991**, *161*, 69–106.
- [13] P. Knops, N. Sendhoff, H.-B. Meikelburger, F. Vögtle, *Top. Curr. Chem.* **1991**, *161*, 2–36.
- [14] J. Bobacka, T. Lahtinen, J. Nordman, K. Rissanen, A. Lewenstam, A. Ivaska, *Electroanalysis* **2001**, *13*, 723–726.
- [15] J. Bobacka, T. Lahtinen, H. Koskinen, K. Rissanen, A. Lewenstam, A. Ivaska, *Electroanalysis* **2002**, in press.
- [16] P. Saarenketo, R. Suontamo, T. Jödicke, K. Rissanen, *Organo-metallics* **2000**, *19*, 2346–2353.
- [17] P. Saarenketo, R. Suontamo, K. Rissanen, *Organometallics* **2002**, submitted.
- [18] F. Vögtle, *Justus Liebigs Ann. Chem.* **1969**, *728*, 17–20.
- [19] P. Jessup, J. Reiss, *Aust. J. Chem.* **1976**, *29*, 1267–XXXX.
- [20] H. Hopf, F. Heirtzler, P. G. Jones, P. Bubenitschek, V. Lehne, *J. Org. Chem.* **1993**, *58*, 2781–2784.
- [21] F. Heirtzler, H. Hopf, P. Bubenitschek, P. G. Jones, *Tetrahedron Lett.* **1995**, *36*, 1239–1242.
- [22] P. G. Jones, P. Bubenitschek, F. Heirtler, H. Hopf, *Acta Crystallogr., Sect. C* **1996**, *52*, 1380–1384.
- [23] P. G. Jones, F. Heirtzler, H. Hopf, *Acta Crystallogr., Sect. C* **1996**, *52*, 1384–1388.
- [24] J. J. P. Stewart, *J. Comput. Chem.* **1986**, *10*, 209–XXXX.
- [25] SPARTAN, Version 5.0.2, Wavefunction Inc., Irvine, CA, **1991–1997**.
- [26] M. J. Frisch, G. W. Trucks, H. B. Schlegel, G. E. Scuseria, M. A. Robb, J. R. Cheeseman, V. G. Zakrzewski, J. A. Montgomery, Jr., R. E. Stratmann, J. C. Burant, S. Dapprich, J. M. Millam, D. Daniels, K. N. Kudin, M. C. Strain, O. Farkas, J. Tomasi, V. Barone, M. Cossi, R. Cammi, B. Mennucci, C. Pomelli, C. Adamo, S. Clifford, J. Ochterski, G. A. Petersson, P. Y. Ayala, Q. Cui, K. Morokuma, D. K. Malick, A. D. Rabuck, K. Raghavachari, J. B. Foresman, J. Cioslowski, J. V. Ortiz, B. B. Stefanov, G. Liu, A. Liashenko, P. Piskorz, I. Komaromi, R. Gomperts, R. L. Martin, D. J. Fox, T. Keith, M. A. Al-Laham, C. Y. Peng, A. Nanayakkara, C. Gonzalez, M. Challacombe, P. M. W. Gill, B. Johnson, W. Chen, M. W. Wong, J. L. Andres, C. Gonzalez, M. Head-Gordon, E. S. Replogle, and J. A. Pople: GAUSSIAN 98, Revision A.6, Gaussian Inc., Pittsburgh PA, **1998**.

Received March 15, 2002  
[O02155]